I.A.Shuklov, V.F.Razumov
Russ. Chem. Rev., 2020, **89** (3) 379 – 391

https://doi.org/10.1070/RCR4917

Lead chalcogenide quantum dots for photoelectric devices

Ivan A. Shuklov [a], Vladimir F. Razumov [a, b]

[a] *Moscow Institute of Physics and Technology, Institutskiy per. 9, 141701 Dolgoprudny, Moscow Region, Russian Federation*
[b] *Institute of Problems of Chemical Physics, Russian Academy of Sciences, prosp. Akademika Semenova 1, 142432 Chernogolovka, Moscow Region, Russian Federation*

The review concerns the state of the art in methods of synthesis of colloidal lead chalcogenide quantum dots (QDs). The most recent data on the mechanisms of chemical transformations involving various precursors are discussed. Particular attention is paid to the influence of (i) trace impurities in the reactants used and (ii) post-synthesis treatment on the physicochemical properties of QDs used in photoelectric devices.
The bibliography includes 129 references.

Contents

1. Introduction 379
2. Syntheses of colloidal PbSe quantum dots 381
2.1. Syntheses using trioctylphosphine 381
2.1.1. The influence of impurities 382
2.1.2. The morphology of PbSe nanoparticles 382
2.2. Syntheses using oleylamine 383
2.3. Syntheses based on cation exchange 383
2.4. Syntheses in aqueous media 384
2.5. Alternative sources of selenium 384
3. Ligand exchange 385
4. Mixed chalcogenides $PbS_{1-x}Se_x$ and $PbSe_{1-x}Te_x$ *387*
5. Surface passivation of colloidal PbSe quantum dots 387
6. Applications of colloidal PbSe quantum dots 388
7. Conclusion 389

1. Introduction

Unique electronic and optical properties of lead chalcogenides (PbS, PbSe and PbTe) have made them basic optoelectronic materials as long as several decades ago. The first infrared (IR) PbS photodetectors were fabricated in the 1930s. Thin layers of polycrystalline lead chalcogenides were used in IR sensors during World War II. Mass production of infrared PbS and PbTe photodetectors for warheads of target-seeking air-to-air missiles began in the USA in the 1950s.

The development of cryogenic cooling technologies led to a considerable increase in the sensitivity of IR detectors and to wide application of these devices in scientific research. In the mid-1960s researchers at the Mount Wilson observatory (USA) for the first time conducted a near-IR survey of the sky using cooled PbS photodetectors and detected more than 20 000 sources of IR radiation. Since then, there has been rapid progress in the studies on space objects visible in the IR spectral range. With the advent of space observatories in the 1980s, researchers began to explore the mid-IR and far-IR ranges that appeared to be highly informative for astronomers who detected previously unknown sources of radiation. Thus a new branch of science called IR astronomy was born.

In the last two decades, considerable efforts have been made to improve the characteristics of the available photodetectors, to simplify the production technology and to markedly increase the operating temperatures. As a consequence, new promising structures were engineered and new technologies developed. Among the former, there are quantum dot IR detectors.

I.A.Shuklov. Doctor rerum naturalium, Senior Researcher at MIPT. Telephone: +7(495)408 – 4554, e-mail: shuklov.ia@mipt.ru
V.F.Razumov. Corresponding Member of the Russian Academy of Sciences, Doctor of Sciences (Physics and Mathematics), Professor, Head of Laboratory for Photonics of Quantum Nanostructures at MIPT and Head of Laboratory of Photonics of Nanosized Structures at IPCP RAS. Telephone: +7(49652)21 – 288, e-mail: razumov@icp.ac.ru
Current research interests of the authors: nanosystems and nanomaterials, development of new methods for the synthesis of nanoparticles, studies on self-assembly of ordered supramolecular and hybrid nanostructures, design of novel functional nanomaterials for data regeneration systems, electroluminescent and photovoltaic devices and sensors.

Translation:A.M.Raevskiy

Received 7 August 2019

© 2020 Uspekhi Khimii, ZIOC RAS, Russian Academy of Sciences and IOP Publishing Limited

Table 1. Main physical properties of lead chalcogenides.[3–6]

Chalcogenide	r_B/nm	Band gap /eV		ε_r (see [a])
		bulk sample at 300 K	CQDs	
PbS	18	0.41	0.6–1.6	17.2
PbSe	46	0.28	0.35–1.7	23
PbTe	150	0.31	0.6–1.1	33

[a] Relative dielectric constant.

The term 'quantum dot' (QD) was introduced in 1988 to describe ultradispersed particles that exhibit the quantum size effect.[1] In 1993, a synthetic route to the production of colloidal QDs (CQDs) was proposed; it was called high-temperature colloidal synthesis.[2] The method affords CQDs of specified size with minimum dispersion of the particle size distribution function (to 5%). The next 25 years of intensive research into CQDs yielded significant results.

This review highlights the most important methods for the synthesis of colloidal lead chalcogenide QDs, a promising type of QDs exhibiting an excellent photosensitivity in the near-IR and mid-IR ranges and having band gaps in the range of 0.3 to 2.0 eV. The combination of broadband absorption and large Bohr exciton radius (r_B) of these compounds (Table 1) make them candidates for application in lasers, telecommunications devices, solar cells, photodetectors and electroluminescent devices.

The main part of the review is devoted to the synthesis methods and the physicochemical properties of colloidal PbSe QDs that underlie their applications in photoelectric devices operating in the near-IR and mid-IR ranges. From the data in Table 1 it follows that PbSe has the widest range of band gap tuning. This property is crucial to the design of photodetectors. To date, chemistry of colloidal PbSe QDs is less studied than chemistry of colloidal PbS QDs.

Photoelectric devices based on colloidal PbSe QDs have a great potential and are competitive with the widely used devices based on polycrystalline PbSe and epitaxial PbSe layers.[3] Certain devices based on colloidal PbSe QDs are characterized by lower dark current, higher operating temperature and threshold sensitivity;[7,8] they also proved themselves in semiconductor lasers.[9,10] Large Bohr exciton radii and small effective masses of electrons and holes in films of colloidal lead chalcogenide QDs favour charge delocalization. A direct consequence is high electron mobility in thin films of colloidal PbSe QDs. For instance, an electron mobility of 0.95 $cm^2\ V^{-1}\ s^{-1}$ was determined for films fabricated from close-packed colloidal PbSe QDs treated with a hydrazine solution.[11]

Colloidal PbSe QDs are of particular interest for production of solar cells because they exhibit the multiple exciton generation effect,[12–14] *i.e.*, multiple exciton generation upon absorption of a photon with energy much exceeding the band gap. The colloidal PbSe QD solar cells have a potential to overcome the Shockley–Queisser theoretical limit equal to 33.7% and thus to increase the efficiency of solar energy conversion.[15] An external quantum yield of 300% due to the multiple exciton generation in colloidal PbSe QDs was reported.[13] The effect was observed in real solar cells.[16]

Colloidal PbSe QDs are characterized by more efficient multiple exciton generation than colloidal PbS QDs. Therefore, it is colloidal PbSe QDs that allow one to design more efficient devices.

Natural lead sulfide and lead selenide exist as galena and clausthalite minerals. However, these natural materials are hard to be used for the synthesis of CQDs suitable for production of electronic devices.[17] The synthesis of colloidal PbS and PbSe QDs requires special procedures (which, however, are applicable to the preparation of other CQDs).[18] Methods used in chemistry of PbS and PbSe are analogous and in most cases readily transferable from one chalcogenide to another.

Lead selenide has a relatively large Bohr exciton radius; therefore, the properties of colloidal PbSe QDs depend strongly on the particle size. A correlation between the band gap and the size of spherical PbSe particles is shown in Fig. 1.

An empirical formula relating the band gap (E_0) to the QD diameter (d) was proposed. It is based on the published experimental data, gives a good approximation in the d range from 2 to 20 nm and has the form

$$E_0 = 0.278 + \frac{1}{0.016\,d^2 + 0.209\,d + 0.45} \quad (1)$$

A simplified linear relation between the diameter of colloidal PbSe QD and the position of the first exciton absorption peak (wavelength λ) provides a quite good approximation[20] of experimental data in the particle size range from 3 to 5.5 nm:

$$d = \frac{\lambda - 143.75}{281.25} \quad (2)$$

A number of reviews on certain aspects of the synthesis, application and chemistry of colloidal PbSe QDs have been reported in the last 15 years. Core–shell heterostructures with the PbSe core for optoelectronic applications were considered,[21] as well as photovoltaic devices based on colloidal lead chalcogenide QDs and methods of synthesis of these QDs,[22] thermoelectric devices based on colloidal lead chalcogenide QDs,[23] and, eventually, the synthesis and characterization of near-IR emitting CQDs.[24] Up to our

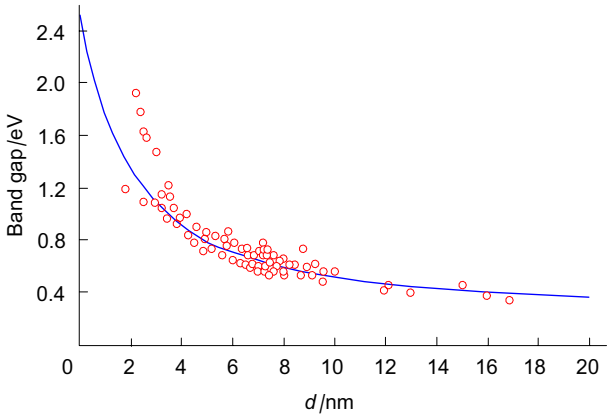


Figure 1. Correlation between the band gap and diameter of spherical PbSe particles plotted using published and experimental data.[19]

knowledge, there is no review article that (i) gives a holistic view of the synthesis and possible modifications of colloidal lead chalcogenide QDs (especially, PbSe QDs) irrespective of the final field of application and (ii) contains comprehensive information on chemistry of precursors used in the synthesis. We hope this review will not only bridge the gap, but also help researchers in their search for novel methods for the synthesis of colloidal lead chalcogenide QDs aimed at producing photodetectors with improved properties.

The list of notations and abbreviations used in this review is as follows:

CQDs — colloidal QDs,
DMF —*N*,*N*-dimethylformamide ,
DPP — diphenylphosphine,
DPPSe — diphenylphosphine selenide,
OA — oleic acid,
ODE — octadecene,
OLA — oleylamine,
PMMA — poly(methyl methacrylate),
TOP — tri-n-octylphosphine,
TOPSe — tri-n-octylphosphine selenide.

2. Syntheses of colloidal PbSe quantum dots

Dozens of methods for the synthesis of PbSe QDs from various sources of lead and selenium have been developed to date. They can be divided into two groups. One group of methods uses a single source of selenium and lead, while the other uses two different sources (selenium and lead compounds). The latter approach is more popular because it allows one to vary the lead/selenium ratio in the reaction mixture.

Most often, the sources of selenium include tri-n-octylphosphine selenide (TOPSe) and elemental selenium in oleylamine; the sources of lead include lead halide (PbX_2, X = Cl, Br, I) solutions in oleylamine and lead oleate, which is obtained by dissolving lead acetate or lead oxide in oleic acid.

Recently, there has been increasing interest in the synthesis of lead chalcogenide QDs by substitution of lead atoms for cadmium, silver, zinc and other metal cations in the corresponding metal chalcogenide QDs.

2.1. Syntheses using trioctylphosphine

Usually, tri-n-octylphosphine (TOP) plays a dual role in the synthesis of colloidal PbSe QDs, *viz*., it can form a ligand shell surrounding a CQD to prevent coagulation of colloidal solutions and act as precursor of selenium sources. Syntheses of CQDs using TOP were reported for all three lead chalcogenides, that is, PbS,[25] PbSe[26] and PbTe.[27] This approach is also suitable for the synthesis of other selenide CQDs, *e.g*., colloidal CdSe QDs.[28, 29] In the reaction of TOP with elemental selenium, phosphorus is oxidized to P^V, and a corresponding tri-n-octylphosphine selenide (n-Oct_3PSe) is formed. The solution of n-Oct_3PSe in n-Oct_3P is commonly used as reactant. Like most trialkylphosphines, TOP is readily oxidized by atmospheric oxygen and therefore the syntheses using TOP are carried out in inert atmosphere.

Octadecene (ODE) or diphenyl ether are used as high-boiling solvents. Often, the syntheses of colloidal PbSe QDs are carried out in the presence of diphenylphosphine (DPP). A number of reaction mechanisms involving TOP and diphenylphosphine were proposed. Following the first mechanism established from ^{31}P NMR data, n-Oct_3PSe reacts with Pb^{2+} to give n-Oct_3PO and oleic anhydride, and lead does not change its oxidation state upon the formation of PbSe (Scheme 1).[30]

The reaction in the presence of diphenylphosphine or trace amounts of other secondary phosphines proceeds by the mechanism shown in Scheme 2.

Yet another mechanism involves reduction of Pb^{2+} to Pb^0 by diphenylphosphine and subsequent reaction of Pb^0 with n-Oct_3PSe, which involves re-oxidation of Pb^0 to Pb^{2+} and results in PbSe and TOP.[30, 31] This mechanism is also based on ^{31}P NMR data. Scheme 3 presents the reaction mechanism with changes in the lead oxidation state.[31]

When the reaction is carried out in mixtures of TOPSe with Ph_2PH, the equilibrium is always shifted towards the formation of diphenylphosphine selenide (DPPSe).[32]

$$\text{n-Oct}_3\text{P=Se} + \text{Ph}_2\text{PH} \rightleftharpoons \text{n-Oct}_3\text{P} + \text{Ph}_2\text{P(Se)H} \qquad (1)$$

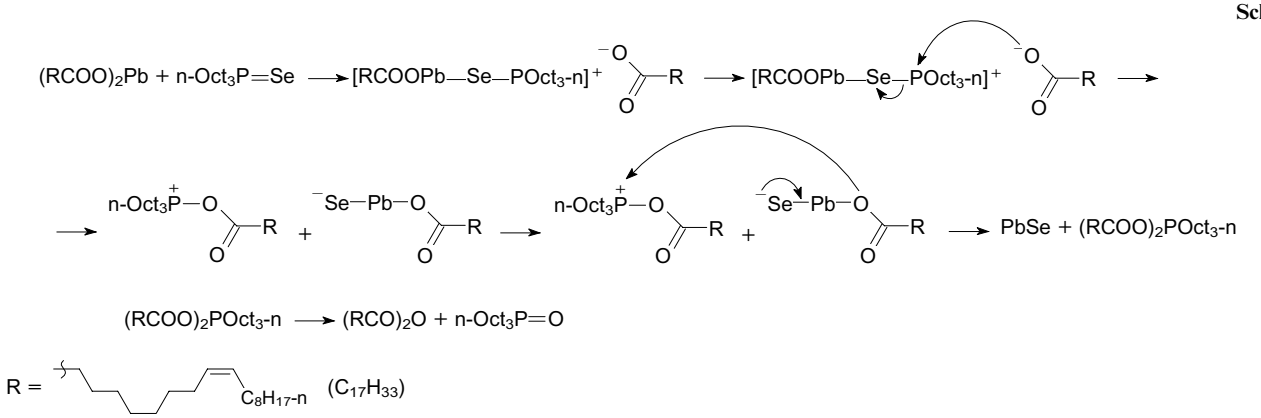
The reaction of DPP with elemental selenium results in $Ph_2P(Se)H$, which rapidly reacts with a solution of lead oleate [$Pb(oleate)_2$] in toluene at room temperature to give PbSe

$$\text{Ph}_2\text{P(Se)H} + \text{Pb(oleate)}_2 \rightleftharpoons \qquad (2)$$

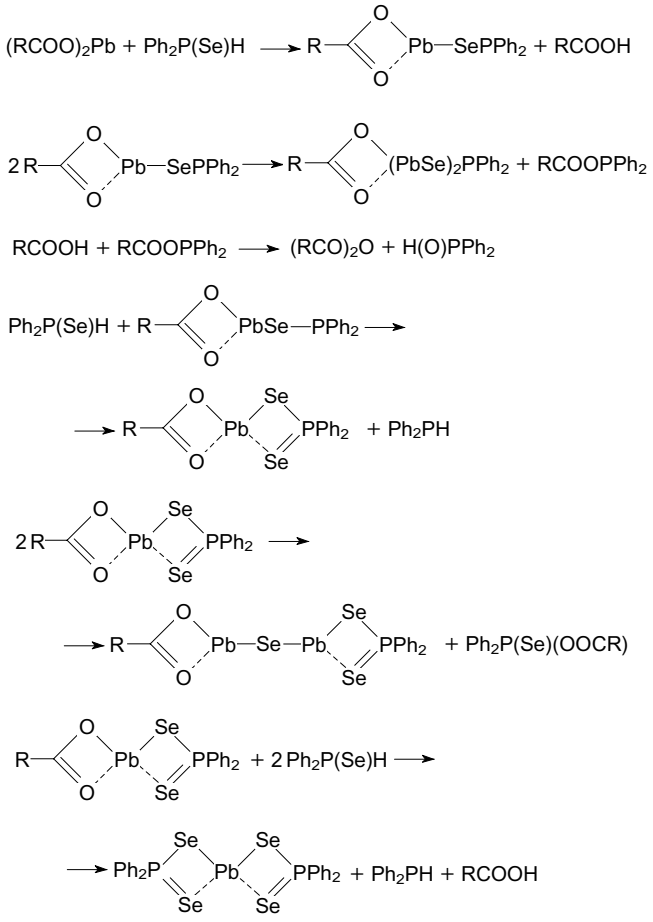
$$\rightleftharpoons [\text{PbSe}]_{\text{colloid}} + \text{side products}$$

A kinetic study on the synthesis of colloidal PbSe QDs showed[33] that the formation of $Ph_2P(Se)H$ is the rate-limiting step of reaction (1). Step (2) is fast and not responsible for the overall reaction rate. A decrease in the reaction rate at high conversions can be explained by the chemisorption of $Ph_2P(Se)H$ onto the surface of colloidal PbSe QDs. It was also established that the reaction rate decreases with

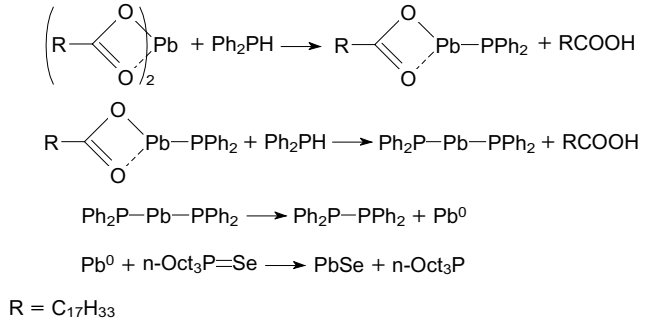
Scheme 1



Scheme 2



Scheme 3



increasing concentrations of oleic acid and n-Oct_3P. This study is a good example of controlling the particle size by varying the reaction rate.

Eventually, diphenylphosphine present in the reaction mixture has a positive effect on nucleation; this is similar to the effect of secondary phosphine impurities in TOP.[34, 35] The addition of Ph_2PH improves the reproducibility of the synthesis of colloidal PbSe QDs owing to compensation of different-quality technical TOP used in the syntheses. The amount of dioctylphosphine as impurity in commercially available TOP can vary over a wide range.

The amount of DPPSe in the reaction mixture determines the concentration of seeds. If the concentration of DPPSe is lower than that of TOPSe, larger colloidal PbSeQDs are formed. The method allows one to prepare CQDs with the first exciton absorption peak in the range of 1500 – 2000 nm. A drawback of this technique consists in broad particle size distribution of the large and small CQDs. The growth of QDs can be controlled by varying the DPP/TOP ratio.[36]

A classical synthesis using n-Oct_3PSe is carried out at 90 – 220 °C. To a solution of lead oleate, a solution of TOPSe in TOP is added.[26] The synthesis of PbSe QDs using n-Oct_3PSe and Ph_2PH at lower temperatures (50 – 90 °C) affords small CQDs (3 – 7 nm in size) characterized by the first exciton absorption peak in the range from 1045 to 1239 nm.[37]

Colloidal PbSe QDs 1 – 1.8 nm in size can be synthesized at 30 °C.[38] By slowly adding a mixture of lead and selenium sources to a hot solution of pre-formed PbSe nanoparticles, one can synthesize CQDs with the first exciton absorption peak pushed to 3400 nm.[39]

Recently, yet another mechanism of formation of colloidal selenide QDs was proposed based on ^{77}Se NMR data. It involves the formation of hydrogen selenide in the reaction of n-Oct_3PSe with oleic acid at temperatures $\geqslant$ 250 °C.[40] It is assumed that H_2Se is the true selenium precursor in the synthesis of colloidal CdSe QDs. However, it remains unclear whether (i) this mechanism can be extrapolated to the synthesis of PbSe that occurs at lower temperatures and (ii) this mechanism is the main route to colloidal metal selenide QDs.

2.1.1. The influence of impurities

Small impurities in the starting reactants used for the synthesis of QDs can have either positive or negative effect on the result of the synthesis. For instance, commercially available trioctylphosphine used to synthesize lead selenide and cadmium selenide contains di-n-octylphosphine oxide and di-n-octylphosphinic acid as impurities. These compounds can significantly influence the morphology of colloidal CdSe QDs. [41]

The presence of di-n-octylphosphine impurity is critical to nucleation.[31] This secondary phosphine is formed as a result of disproportionation of di-n-octylphosphine oxide, a common impurity in TOP. The synthesis of lead or cadmium selenides using tri-n-octylphosphine containing no di-n-octylphosphine at 120 °C is impossible. Contrary to this, the reaction using commercially available tri-n-octylphosphine takes a few minutes under identical conditions.

2.1.2. The morphology of PbSe nanoparticles

Colloidal PbSe QDs up to 9 nm in size have a spherical shape. As the nanoparticle size increases, spheres are transformed into cubes and truncated cubes. Cubic PbSe nanoparticles from 14 to 27 nm in size were synthesized following a conventional procedure using n-Oct_3PSe.[42]

Lead selenide nanowires are formed as main structures (> 95%) at low concentrations of surfactants (oleic acid), high temperatures (200 – 250 °C) and Pb : Se ratios in the range from 1 : 1 to 3 : 1. The addition of a co-surfactant (hexadecylamine) leads to formation of zigzag nanowires or star-shaped particles.[43, 44] By varying the medium, temperature and oleic acid concentration, one can synthesize star-shaped, octahedral, or ring-shaped PbSe nanocrystals. The dependence of the shape of nuclei of colloidal PbSe QDs on the concentration of oleic acid is illustrated in Fig. 2.[44]

Summing up, by varying the particle size, surfactant and co-surfactant, the Pb : Se ratio and the synthesis temper-

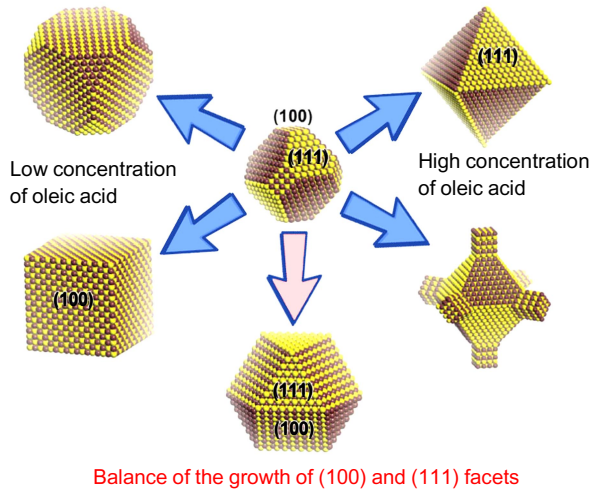


Figure 2. Influence of the concentration of oleic acid on the shape of nuclei of colloidal PbSe QDs.[44]

ature, one can obtain PbSe nanoparticles of different shapes.

2.2. Syntheses using oleylamine

Oleylamine (OLA) used in the synthesis of CQDs can act as:

— high-boiling solvent;

— surface-passivating ligand for the CQD shell;

— long-chain surfactant to stabilize a colloidal solution of CQDs; and

— precursor of selenium or sulfur sources.

Most often, CQDs are synthesized using technical oleylamine containing the *trans*-isomer, unsaturated amines, short-chain amines and luminescent impurities. The effect of purification of oleylamine on the solubility of lead halides and on the results of syntheses of certain CQDs was analyzed.[45]

A mixture of oleylamine with elemental (grey) selenium serves a selenium precursor in the synthesis of PbSe. The use of such a mixture is the second most common approach to the synthesis of colloidal PbSe QDs. Hou *et al.*[46] studied the structures of reaction products of oleylamine with selenium (Scheme 4). These products differ from products of a similar reaction between sulfur and oleylamine.[47] As far as we know, the synthesis of tellurides following this scheme has not been reported. The reaction of oleylamine with selenium involves the addition of Se to the double bond to give selenium-containing monomers and dimers.

The synthesis of colloidal PbSe QDs is analogous to that of colloidal PbS QDs proposed by Cademartiri *et al.*[48] To a solution of $PbCl_2$ in oleylamine, a mixture prepared by dissolving selenium in oleylamine is added at 160 – 200 °C. Following this route, one can obtain colloidal PbSe QDs from 3.6 to 13.9 nm in size.[49, 50]

The synthesis in the presence of dodecanethiol on lowering the temperature to 65 – 80 °C afforded PbSe particles about 3 nm in size having a photoluminescence peak at 950 nm.[51] The fluorescence intensity was dependent on the ratio of the sources of lead and selenium and considerably decreased as the Pb : Se ratio changed from 10 : 0.1 to 10 : 2. Also, the Pb : Se ratio had little effect on the particle size and on position of the photoluminescence peak (from 911 to 950 nm).

The role of oleylamine was studied in some cases only fragmentarily, *viz.*, oleylamine can act as ligand, but one cannot rule out that it also behaves as selenium carrier. For instance, a selenium precursor obtained from octadecene and selenium[52] was used to synthesize colloidal PbSe QDs in oleylamine.[52, 53] However, the issue whether oleylamine is only a ligand or it is involved in the reactions resulting in colloidal PbSe QDs was not studied.

Colloidal PbSe QDs were also synthesized[53] using lead acetylacetonate in oleylamine and selenium powder dissolved in octadecene (Se – ODE). The particle size was temperature dependent and changed from 6.5 nm at a reaction temperature of 120 °C to 8.3 nm at 180 °C. In addition, Pb(OH)Cl nanowires in oleylamine can act as lead precursor in the reaction with a solution of selenium in ODE at 240 °C resulting in larger colloidal PbSe QDs.[54]

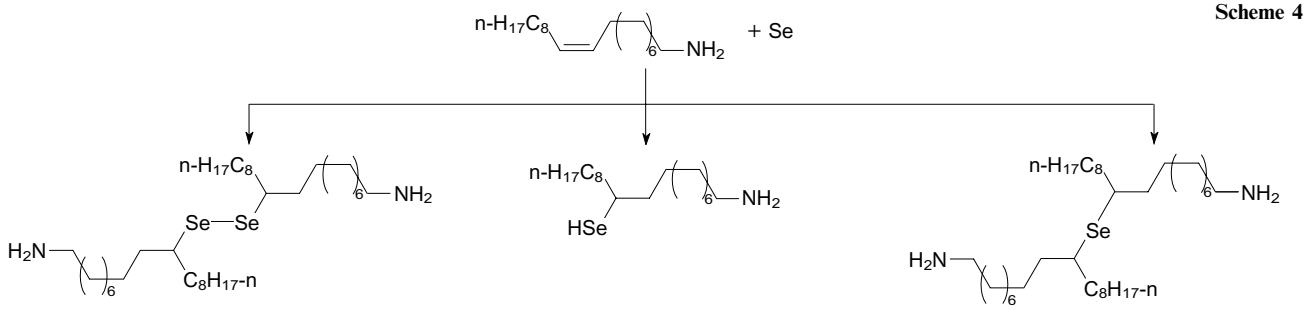
2.3. Syntheses based on cation exchange

Metal ion CQDs can play the role of starting reactants in the synthesis of CQDs by cation or anion exchange. Unlike ion exchange in solids, the process in nanoparticles is rather fast, and its thermodynamics is governed by the coordination of cations or anions in solution. In the last decade, this approach was most widely used to synthesize various QDs.[55] Usually, cation exchange reactions are carried out, anion exchange being less studied.

In the course of ion diffusion and cation exchange the anion sublattice remains relatively stable. As a consequence, anisotropic nanocrystals retain their shape upon cation exchange provided that the smallest QD size is larger than the maximum size of the reaction zone during the exchange process. There is also a topotactic relation between the starting reactants and products. Thus, if the cation exchange reaction is confined within a certain domain of a nanoparticle, different-composition heterostructures thus formed have the same anion sublattice.

Cation exchange was for the first time used to synthesize colloidal PbS QDs from CdS in 2009.[56] The substitution of silver cations by lead cations in colloidal spheres Ag_2Se@Se

Scheme 4



(selenium core is coated with a silver selenide shell) was for the first time reported in 2007.[57] In 2014, PbSe QDS were synthesized using this approach.[58] It was shown that the process can be started with colloidal CdSe QDs. The exchange occurred at 150 °C following injection of a solution of colloidal QDs CdSe in octadecene into a solution of $PbCl_2$ in oleylamine. Colloidal PbSe QDs thus formed were characterized by high stability to oxidation in air because the CQD facets prone to oxidation were covered with $PbCl_2$. The diameter of the colloidal PbSe QDs thus obtained varied from 2.5 to 4.8 nm. Colloidal PbSe QDs synthesized analogously in another study[59] were used for fabricating an NO_2 sensor.

Colloidal PbSe QDs can also be synthesized from ZnSe QDs.[60]

An interesting approach[61] to the synthesis of colloidal PbSe QDs and PbS with a very narrow particle size distribution involves a combination of cation exchange and Ostwald ripening. It allows one to obtain colloidal PbSe QDs with only 3.6% dispersion of the particle size distribution function. To this end, a solution of 3.3-nm colloidal QDs CdSe in octadecene was injected into a solution of $PbCl_2$ in oleylamine at 190 °C. Then the temperature was lowered to 160 °C, the reaction mixture was kept at this temperature for some time and 1.9-nm colloidal CdSe QDs were added in small portions. In this case the growth of large PbSe QDs was promoted by the dissolution of smaller colloidal PbSe QDs formed from colloidal CdSe QDs in the excess amount of $PbCl_2$. Colloidal PbSe QDs thus obtained had the first exciton absorption peak in the wavelength range of 1.3 to 2.2 μm.

Cation exchange in the nucleation stage followed by Ostwald ripening provides a convenient synthetic route to colloidal PbSe QDs.[62] Tin selenide nuclei formed in the reaction of $Sn[N(SiMe_3)_2]_2$ with TOPSe were introduced into the reaction with $PbCl_2$ in oleylamine at 140 – 160 °C. The method was used to prepare a series of monodisperse samples of colloidal PbSe QDs (Fig. 3). Retention of the morphology of the starting nanocrystal upon cation exchange and stoichiometric control of the reaction course provides QDs with composition, morphology and crystalline phases inaccessible by other methods.

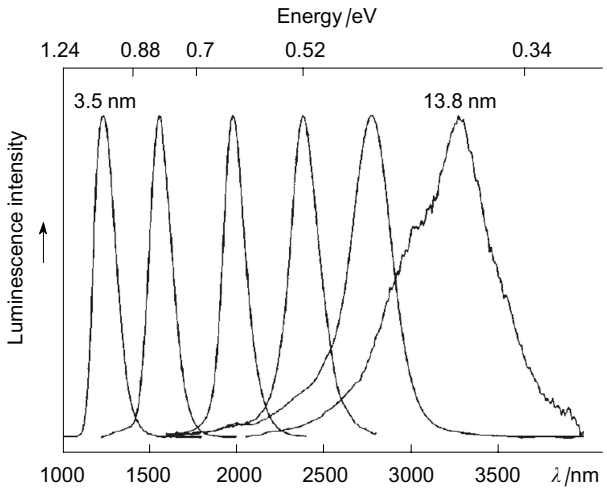


Figure 3. Luminescence spectrum of colloidal PbSe QDs in tetrachloroethylene (λ_{exc} = 980 nm).[62] The QD diameters were from 3.5 to 13.8 nm.

2.4. Syntheses in aqueous media

Colloidal PbSe QDs can be synthesized in aqueous media. This approach is of particular interest for fabrication of water-soluble nanoparticles for medical applications. The starting compounds were lead acetate [$Pb(OAc)_2$] and Na_2SeSO_3,[63 – 65] SeO_2 and $N_2H_4 \cdot 2\,HCl$,[65] and gaseous H_2Se.[66] Soluble starch[63] and citrate ions[63, 64] were used as ligands to form the CQD shell; as a result, nanoparticles at least 20 nm in diameter were prepared. Colloidal particles less than 10 nm in size synthesized using these techniques appeared to be unstable in aqueous media. A transmission electron microscopy study[65] revealed the formation of CQDs 5 – 10 nm in size when using thiocarboxylic acids.

The reaction of $Pb(OAc)_2$ with Na_2SeSO_3 resulted in PbSe particles from 26 to 33 nm in size with band gaps from 2.1 to 1.96 eV depending on the synthesis temperature, which was varied from 328 to 343 K.[66]

Colloidal PbSe QDs can be synthesized by irradiating a mixture of lead and selenium sources prepared by reducing $SeCl_4$ and $Pb(NO_3)_2$ in the presence of $NaBH_4$ with a 532-nm pulsed Nd laser.[67] The method was used to synthesize nanoparticles from 7 to 28 nm in size with a broad particle size distribution (polydispersity index varied from 0.13 to 0.24).

Unfortunately, the photoluminescence properties of particles synthesized using the methods considered above are poorly studied. This is probably due to low quantum yields of luminescence when the synthesis is carried out in aqueous media.

2.5. Alternative sources of selenium

The sources of selenium are not limited to tri-n-octylphosphine selenide and the mixture of oleylamine and selenium, but also include other compounds that are of limited use.

Often, colloidal PbS QDs are synthesized using bis(trimethylsilyl) sulfide as sulfur precursor.[68] A similar synthesis of colloidal PbSe QDs from bis(trimethylsilyl) selenide[69] is not widely used, probably, due to high cost and low stability of the compound in air.

N,*N*,*N*′-Trisubstituted selenourea derivatives can be obtained with ease by the reaction of selenium, isocyanide and primary amines. These compounds are of interest for the synthesis of colloidal PbSe QDs. This approach was for the first time demonstrated in the synthesis of PbSe nanowires using *N*,*N*-diethyl-*N*′-naphthoylselenourea as selenium precursor.[70] Using other trisubstituted selenoureas and having optimized the synthetic procedure, colloidal PbSe QDs with band gaps from 0.6 to 2.0 eV were prepared.[71] In this case the nanoparticle size depends on the substituted selenourea used as precursor and on the synthesis temperature (from 60 to 120 °C). The photoluminescence properties of the nanoparticles were not studied.

Selenium dioxide in octadecene was proposed as alternative to elemental selenium in octadecene. This mixture is characterized by high stability to atmospheric oxygen; however, SeO_2 is more toxic than elemental selenium. The new precursor was used to synthesize colloidal CdSe QDs with narrow particle size distribution for subsequent photoluminescence study;[72] it was also shown that the method is suitable for the synthesis of colloidal PbSe QDs.

Colloidal PbSe QDs of different morphology were prepared[73] from Ph_4Pb and Ph_3PSe in oleylamine at 220 °C. The shape of nanoparticles was dependent on the solvents and surfactants and on the solvent/surfactant ratio in the reaction mixture. Also, cycloocteno-1,2,3-selenadia-

Table 2. Main methods of synthesis of colloidal PbSe QDs.

Compounds used for the synthesis of precursors		Surfactant	T /°C	Average CQD diameter /nm	Exciton peak maximum /μm	Ref.
lead	selenium					
$PbCl_2$, OLA	DPPSe, TOPSe, DPP, TOP	ODE	30 – 160	2 – 6	0.75 – 2.10	36
PbO, OAH	TOPSe, DPP, TOP	Hexadecane	80 – 145	2 – 5	1.00 – 1.80	33
PbO, OAH	TOPSe, TOP	ODE	30	1 – 1.8	0.70 – 0.88	38
$PbCl_2$, OLA	TOPSe, TOP	Ph_2O	90 – 220	3 – 9	2.50 – 3.40	39
$PbCl_2$, OLA	OLA, Se	–	180 – 220	7.5 – 15	1.70 – 2.10	49
$PbCl_2$, OLA	OLA, Se	–	140 – 240	4.4 – 12.1	–	50
$Pb(acac)_2$	ODE, Se	DA, OLA [a]	120 – 180	6.5 – 16	–	53
$PbCl_2$, OLA	CdSe QDs	ODE	150 – 180	2.5 – 4.8	0.85 – 1.49	58
$PbCl_2$, OLA	CdSe QDs, TOPSe	ODE	180	> 5	1.90	58
Lead complexes with selenoureas		Octene-1, diglyme [a]	100	1.7 – 6.6	0.90 – 2.00	71

Note. Notations are as follows: OLA is oleylamine; OAH is oleic acid; DPPSe is diphenylphosphine selenide; DA is decanoic acid and acac is acetylacetonate; TOP is tri-n-octylphosphine, ODE is octadecene.
[a] Solvent.

zole seems to be yet another possible alternative to traditionally used selenium precursors.[74]

Thus, modern methods of synthesis allow one to prepare colloidal PbSe QDs from 1 to 16 nm in size with the first exciton absorption peak in the range of 700 to 3400 nm (Table 2). A particular method is chosen depending on the available laboratory equipment and on the demand for nanoparticles with absorption in a certain spectral range.

3. Ligand exchange

The ligand shell of any QDs directly affects their optical, electrical and catalytic properties as well as the ability to form colloidal solutions in various media.[75] According Owen, ligands in nanoparticles are divided into the following three classes, each core – ligand bond being formally treated as covalent one:[76]

1) L-type ligands — neutral two-electron donor ligands (amines, phosphines, phosphine oxides);

2) X-type ligands — anionic ligands [*e.g.*, $RCOO^-$, $RP(O)O^-$, Cl^-, HO^-] or neutral radicals with odd number of electrons. Both subtypes seemingly donate an electron to form a chemical bond;

3) Z-type ligands — electron-withdrawing ligands that withdraw two electrons from the core and coordinate to free electron-rich atoms Se, S, Te (*e.g.*, $CdCl_2$, $InCl_3$).

This classification is used in the design of ligand exchange reactions. It provides a good explanation for difficulties reported in the early studies on modification of the ligand shell, *e.g.*, in the exchange of X-type and L-type ligands. The type of a ligand (L, X or Z) dictates possible mechanisms of substitution reactions and the most appropriate media. For instance, L-type ligands can be rapidly adsorbed onto and desorbed from the surface of nanocrystals at room temperature in apolar solvents, whereas X-type ligands remain strongly bound to the core due to electrostatic interaction under identical conditions.

In the case of conventional synthesis of PbSe using oleic acid and tri-n-octylphosphine, the shell of a colloidal QD is mainly composed of oleates (in the presence of a minimum amount of TOP or without TOP).[77 – 79] Various methods were proposed to increase the conductivity of CQD films through a decrease in the thickness of the ligand shell and an increase in the oxidative stability of QDs. The thinner the ligand shell the shorter the inter-particle distance in the films. Both partial or complete exchange of the starting oleates for inorganic and organic ligands were studied. The list of compounds tested as organic ligands includes mono- and bidentate amines,[80 – 82] hydrazine,[11] carboxylic acids,[84 – 86] thiols and dithiols,[87 – 89] benzene-1,4-dithiol [83] and alkylselenol.[90]

A significant problem in the exchange of the oleate (oleylamine) ligand shell formed in course of the synthesis of CQDs for other organic ligands is the completeness of the substitution reaction. Exchange of a ligand shell by another one is an equilibrium reaction (Fig. 4); therefore, the equilibrium can be shifted in one direction or another by increasing the concentration of the substitution ligand or by carrying out the reaction in the substitution ligand medium.

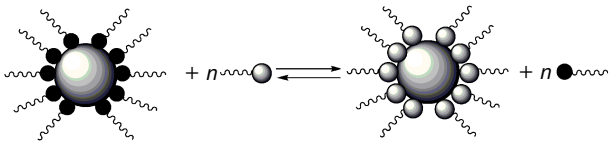


Figure 4. A schematic of equilibrium ligand exchange on the surface of a CQD.

When the oleate shell of CQDs in CQD films is exchanged for such dithiols as ethanedithiol and benzene-1,4-dithiol, the long-chain ligands are replaced by short-chain ones and nanocrystals are cross-linked by these bidentate ligands (Fig. 5).[89] Gradual replacement of oleates by octylamine in solution and then by thiols in films is more preferred due to smaller size difference between the ligands; as a consequence, no cracks appear in the films.

Often, the syntheses of hydrophilic colloidal PbSe QDs in aqueous media give unsatisfactory results, especially in the case of small CQDs (< 20 nm in size). Therefore, these CQDs are prepared by exchange of hydrophobic oleate (oleylamine) ligands for water-soluble ones. For instance, the oleate shell was replaced by L-cysteine in the two-phase system sodium – phosphate buffer – toluene at room temperature. In this case, colloidal PbSe QDs migrated from the organic phase to the aqueous phase. Colloidal PbSe QDs

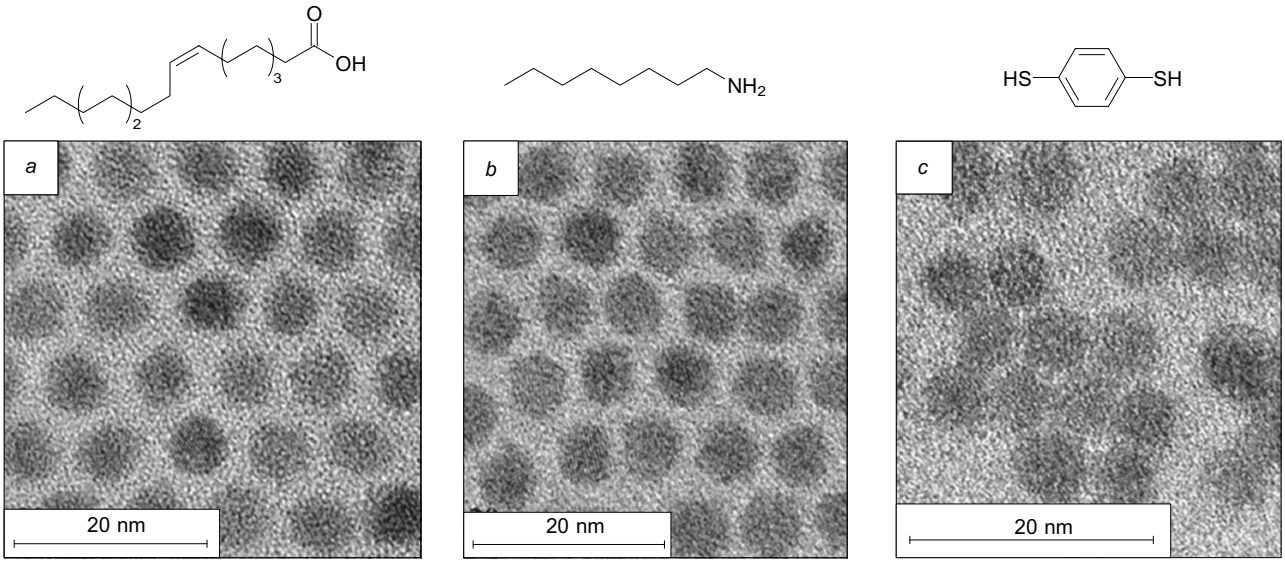


Figure 5. TEM images of films of colloidal PbSe QDs with different ligand shells.[89]
Ligand: oleic acid (*a*), n-octylamine (*b*) and benzene-1,4-dithiol (*c*).

prepared using such an exchange reaction were characterized by a luminescence peak with a maximum at 675 nm.

Usually, inorganic ligands form a thin shell around the semiconductor core (*e.g.*, the shell is ~1 Å thick for S^{2-} and ~21 Å for oleic acid). This allows one to attain strong electronic coupling between QDs in the films, which in turn ensures good conductivity. Inorganic ions can quantitatively replace the starting ligands on the surface of QDs and thus form electrically stabilized colloidal systems in polar solvents.[91] Ideally, this should enable fabrication of conductive CQD films without post-synthesis heat (or chemical) treatment and often without accompanying

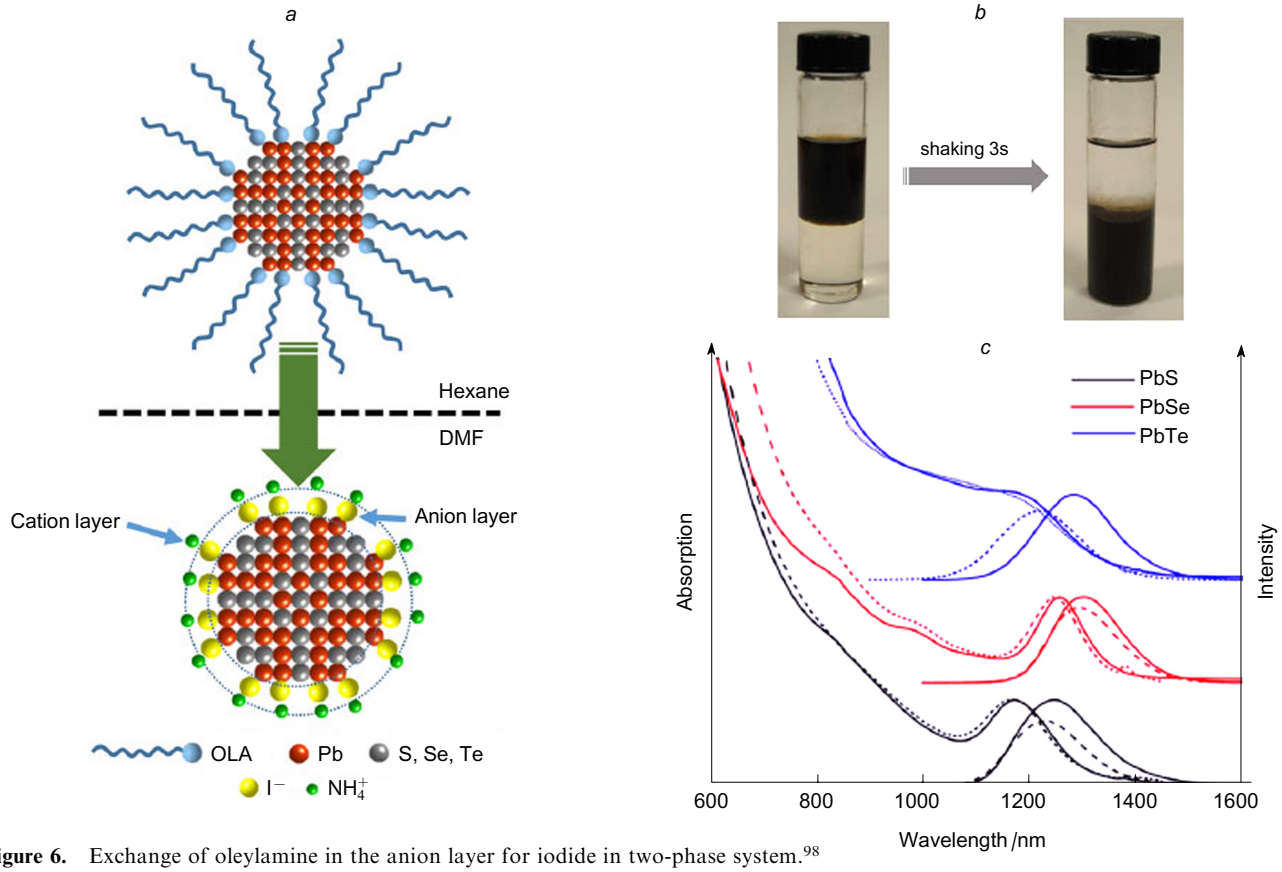


Figure 6. Exchange of oleylamine in the anion layer for iodide in two-phase system.[98]
Schematic diagram of the ligand exchange process in two-phase system (*a*);
photographs of reaction mixture before and after shaking (*b*); and
changes in absorption and luminescence spectra before (solid lines) and after (dashed lines) exchange with LiI (*c*).

increase in the spatial and energy disorder in the films. In practice, heat treatment at 150 – 300 °C remains necessary to attain good conductivity of such systems.

The following systems were tested for ligand exchange in colloidal PbSe QDs: $Sn_2S_6^{4-}$,[92] chalcogenides,[93, 94] halides[95 – 98] and thiocyanates.[98, 99] Ligand exchange can be carried out in solutions, two-phase systems or in films (Table 3).

Table 3. Replacement of oleate shell by inorganic ligands.

Reactant	Ligand	System	Ref.
Na_2S	S^{2-}	Film	92, 93
$(NH_4)_2S$	S^{2-}	Film	94
NH_4SCN	SCN^-	Two-phase system	98, 99
NH_4SCN	SCN^-	Film	98
NH_4SeCN	$SeCN^-$	Two-phase system	99
$(N_2H_5)_4Sn_2S_6$	$Sn_2S_6^{4-}$	Two-phase system	92
NH_4Cl	Cl^-	Single-phase system	95, 96
NH_4Br	Br^-	Single-phase system	95
NH_4I	I^-	Two-phase system	99
NH_4I	I^-	Film	98
LiI	I^-	Two-phase system	99

Treatment of PbSe films with Na_2S solutions leads to complete removal of oleate ligands and improves the oxidative stability of the samples.[93] Oleylamine is replaced by inorganic (I^-, Br^-, SCN^-) and organic ($HCOO^-$) ligands in the reaction in two-phase systems hexane – *N*,*N*-dimethylformamide (DMF) quantitatively and rapidly (Fig. 6).[99] The reaction proceeds under intense shaking of the solution of the initial ligand in hexane and the solution of the substituent salt in DMF over a few seconds at room temperature.

A complete removal of the ligand shell of CQDs, *viz*., oleates or oleylamine, was for the first time demonstrated under the action of $NOBF_4$ in DMF.[100] Meerwein's salt ($[Me_3O]BF_4$) in DMF – acetonitrile mixture,[101] as well as HBF_4 or HPF_6 in DMF[91] can also be used. In all cases, no aggregation of PbSe particles was observed. 'Bare' colloidal PbSe QDs can again react with various ligands, such as oleic acid, oleylamine, hexylamine or poly(vinyl pyrrolidone).[100] This again results in complete replacement of the ligand shell.

Aliphatic alcohols (MeOH, EtOH, Pr^iOH) can replace the oleate ligand shell on the surface of CQDs.[102] Subsequent treatment of the CQDs with oleic acid solutions leads to partial recovery of the oleate ligand shell.

An interesting approach to a decrease in the thickness of the ligand shell of CQDs was reported.[103] Oleate ligands on the surface of colloidal PbSe/CdSe core/shell QDs were replaced by n-octyldithiocarbamate ligands, which can decompose into sulfur and isocyanate at 205 °C. No agglomeration of nanocrystals in the film with the loss of the quantum size properties was observed at this temperature.

4. Mixed chalcogenides $PbS_{1-x}Se_x$ and $PbSe_{1-x}Te_x$

At present, both solid solutions (alloys) of PbSe and PbS, where sulfur and selenium are uniformly distributed in the bulk of nanoparticles, and core/shell structures are known. Either complete or partial replacement of the ligand shell by the inorganic sulfides considered in Section 3 results in structures that can be treated as a PbSe core coated with a PbS shell. Thicker PbS shells can be prepared by growing the second shell on isolated colloidal PbSe QDs or directly in the course of synthesis.[25, 104, 105] For instance, PbSe/PbS nanoparticles were synthesized by adding a solution of colloidal PbSe QDs 3 – 4 nm in size and TOPS to a solution of $Pb(OAc)_2$ and oleic acid in TOP at 180 °C.[105] This resulted in colloidal PbSe QDs coated with 1 – 3 PbS monolayers; the band gap of these CQDs was in the range of 0.8 – 1 eV. Colloidal PbSe QDs coated with the PbS shell demonstrate much higher oxidative stability than colloidal PbSe QDs.[105]

The lattice constants of isostructural crystals PbS and PbSe differ by only 2%. These lead chalcogenides meet the necessary conditions for the formation of solid solutions since their anions are isovalent and their radii differ by less than 15%. The synthesis of mixed chalcogenides $PbS_{1-x}Se_x$ ($0 \leqslant x \leqslant 1$) can involve one, two and even many precursors. When two different precursors of selenium and sulfur are also simultaneously used as reactants, one can prepare alloys of the composition $PbS_{1-x}Se_x$. By varying the reactivity and the ratio of the precursors one can influence the sulfur/selenium ratio in the colloidal $PbS_{1-x}Se_x$ QDs.[106 – 108] For instance, mixed chalcogenides were prepared[106] by adding a mixture of $(Me_3Si)_2S$ with Bu^n_3PSe in octadecene to a lead oleate solution at 150 °C. Owing to reactivity difference between the sulfur and selenium precursors the Se : S ratio in the reaction product was a nonlinear function of the Se : S ratio in the starting reactants. This method was used to synthesize monodisperse 4-nm CQDs with the first exciton absorption peak in the range from 1 to 1.6 μm. The properties of these nanoparticles obeyed Vegard's law, thus being indicative of homogeneous composition of the solid solution. Schottky diodes based on $PbS_{1-x}Se_x$ nanoparticles demonstrated improved properties compared to those of the devices based on pure chalcogenides PbS or PbSe.

The synthesis of $PbS_{1-x}Se_x$ nanoparticles from triphenylphosphine selenide and dibenzyl disulfide as selenium and sulfur precursors in dibenzylamine in the presence of oleic acid affords hexapod crystals.[109] A similar strategy using $(Me_3Si)_2Se$ and Bu^n_3PTe can be utilized to synthesize $PbSe_{1-x}Te_x$.[108, 110]

The synthesis of CQDs by decomposition of a mixture of selenourea and thiourea complexes of lead at 200 °C offers prospects for controlling the selenium/sulfur ratio in the product.[111] The reaction results in large cubic $PbS_{1-x}Se_x$ nanoparticles 25 – 29 nm in size. However, this method dos not allow one to vary the particle size.

Recently, it was proposed to synthesize mixed chalcogenides using cation exchange. An example is provided by the synthesis of colloidal $PbS_{1-x}Se_x$ QDs from colloidal $CdS_{1-x}Se_x$ QDs.[112]

5. Surface passivation of colloidal PbSe quantum dots

Significant drawbacks of colloidal PbSe QDs coated with most organic ligands include the low stability to oxidation by atmospheric oxygen and changes in the luminescence properties (weakening or quenching of luminescence) with time.[94, 113] The oxidation of PbSe on the surface of QDs involves a number of thermodynamically favourable chemical processes listed in Table 4.[114]

Table 4. Gibbs energies (ΔG_{298}) of surface passivation reactions of CQDs.[114]

No.	Reaction	$-\Delta G_{298}$ /kJ mol^{-1}
1	PbSe (s) + 2 O_2 (gas) ⟶ $PbSeO_4$ (s)	405
2	PbSe (s) + 3/2 O_2 (gas) ⟶ $PbSeO_3$ (s)	352
3	PbSe (s) + 3/2 O_2 (gas) ⟶ PbO (s) + SeO_2 (s)	262
4	PbSe (s) + O_2 (gas) ⟶ Pb (s) + SeO_2 (s)	74

Although the formation of $PbSeO_4$ is the thermodynamically most favourable step (see Table 4, reaction *1*), this oxide was not detected in the mixture of room-temperature oxidation products; it follows that reaction *1* requires a higher activation energy. The mixture of the products of oxidation on the surface of PbSe contains SeO_2, PbO and $PbSeO_3$ as major products.[114,115] To improve the oxidative stability, it was proposed to treat the CQDs with chloride,[95–97] bromide[95] or iodide[116,117] solutions. This led to a sharp improvement of this property. As an example, Fig. 7 presents the changes in the absorption spectrum of oleate-coated colloidal PbSe QDs treated with NH_4Cl. Such a treatment causes only partial replacement of the oleate shell at facets that are most prone to the oxidation in air.

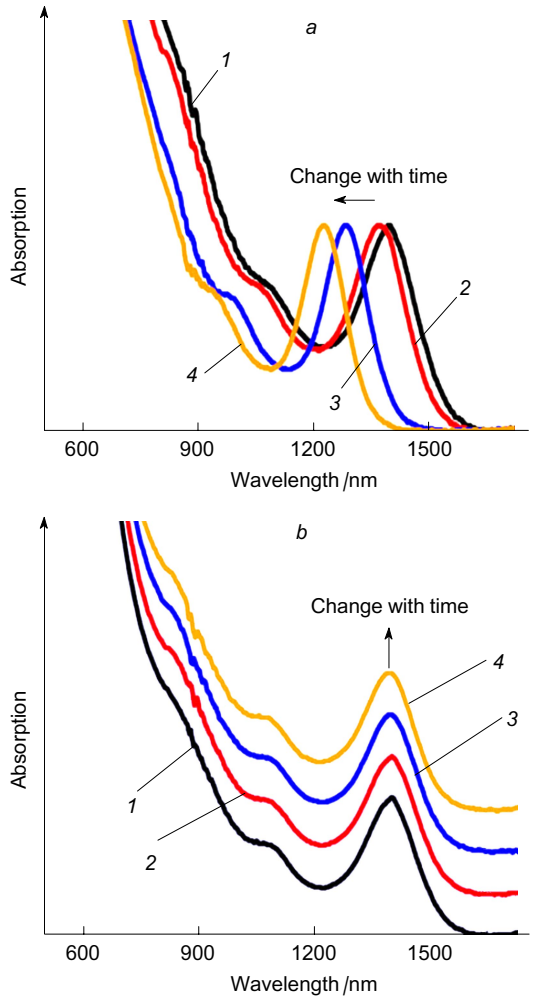


Figure 7. Absorption spectra of oleate-coated colloidal PbSe QDs recorded at different times after synthesis.[95]
Untreated CQDs (*a*) and NH_4Cl-treated CQDs at 0 (*1*), 1 (*2*), 7 (*3*) and 17 days (*4*) after synthesis.

Treatment of QDs with gaseous chlorine was proposed[118] as an alternative to the treatment with ammonium chloride solutions. Lead selenide thus obtained retains the luminescence properties of the untreated sample and exhibits a much higher oxidative stability. Quantum dots can also be treated with a solution of elemental iodine in toluene; in this case the surface lead selenide is transformed to PbI_2.[119]

A study[120] on treatment of colloidal PbSe QDs with cadmium chloride and indium chloride was carried out in order to increase the oxidative stability of these CQDs and to improve the operating properties of solar cells based on them. The most pronounced effect was achieved after treatment of films of colloidal PbSe QDs with a solution of $CdCl_2$ in methanol, *viz.*, the oxidative stability of the films and the open-circuit voltage significantly increased compared to those of the untreated sample. No significant changes in the power conversion efficiency (PCE) of the solar cells based on the treated colloidal PbSe QDs were observed after 270 days of storage in air (Fig. 8).

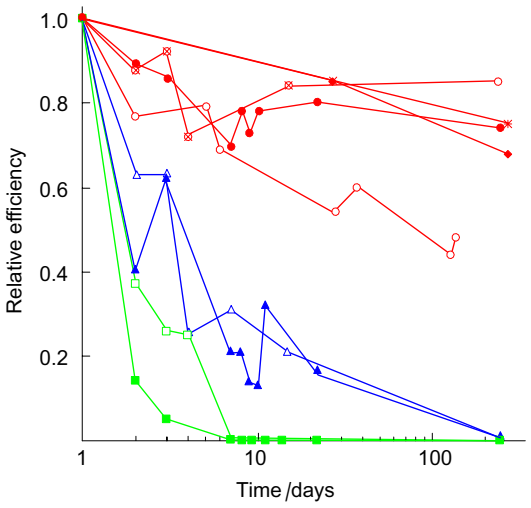


Figure 8. Changes in the relative efficiency of solar cells based on colloidal PbSe QDs in the course of treatment with $CdCl_2$ (red lines) and $InCl_3$ (blue lines) solutions, normalized to the relative efficiency of untreated device (green lines).[120]
Different symbols correspond to different experimental series.

Colloidal PbSe QDs synthesized using $(Et_2N)_3PSe$ as selenium precursor exhibit higher stability to the oxidation by atmospheric oxygen. Based on ^{31}P NMR data, it was shown that surface passivation of the QDs is governed by the products of partial and complete hydrolysis of $(Et_2N)_3P$. This allowed one to propose treatment with alkylphosphonic acids for the QD surface passivation. Indeed, treatment with hexyl-, tetradecyl- and octadecylphosphonic acids improves the stability of colloidal PbSe QDs.[121] Air-stable colloidal PbSe QDs thus prepared can be used to fabricate ambipolar field-effect transistors. This is an undoubtful advantage of this more expensive approach over the surface passivation with halides.

6. Applications of colloidal PbSe quantum dots

Owing to their useful properties, colloidal PbSe QDs have found various application including lasers, telecommunications devices, solar cells, photodetectors and electrolumi-

nescent devices. A number of illustrative examples are given below.

Solar cells based on colloidal PbSe QDs demonstrating high oxidative stability in air were fabricated.[58] These QDs were synthesized from colloidal CdSe QDs by cation exchange. The devices have a typical p – n junction architecture, *viz*., ITO/TiO_2/colloidal PbSe QDs/MoO_3/Al. The main operating parameters of the devices are as follows: a short-circuit current density of 23.4 mA cm^{-2}, a fill factor of 51.9% and a PCE of 6.2%. At present, the maximum PCE of solar cells based on colloidal PbSe QDs is 8.2%; this value was obtained for colloidal PbSe QDs passivated with perovskite $CsPbI_3$.[122]

Near-IR photodetectors based on a nanocomposite comprising poly(3-hexylthiophene-2,5-diyl) (P3HT) and colloidal PbSe QDs were reported.[123] The responsivity and the specific detectivity of a photodetector based on a field-effect transistor Au(gate)/PMMA (930 nm)/P3HT : PbSe (55 nm)/Au(source, drain) were as high as 500 A W^{-1} and 5.02×10^{12} cm $Hz^{-1/2}$ W^{-1} (Jones), respectively. Measurements were carried out at drain – source and gate – drain voltages of −40 V and a laser intensity of 40 mW cm^{-2} under irradiation at $\lambda = 980$ nm.

A near-IR tandem photodetector based on colloidal PbSe QDs and ZnO nanocrystals with a detectivity of 4.7×10^{13} Jones at 275 K was described.[124]

Colloidal PbSe QDs 3 nm in diameter were used for fabrication of nitrogen dioxide sensors, *viz*., colloidal PbSe QDs were coated onto ceramic substrates and treated with a $Pb(NO_3)_2$ solution to remove bulky surface ligands. The sensors were highly sensitive to NO_2 (50 ppm) and had a short response time of 7 s.[59] An acetylene detector based on colloidal PbSe QDs was also reported.[125]

Field-effect phototransistors[126] based on a $MeNH_3PbI_3$ perovskite/colloidal PbSe QD heterojunction demonstrated good external quantum efficiency and PCE. High responsivity of 1.2 A W^{-1} at 460 nm was due to the combination of perovskite and colloidal PbSe QDs. The charge carrier mobility determined for the phototransistor was 0.147 cm^2 V^{-1} s^{-1} for holes and 0.16 cm^2 V^{-1} s^{-1} for electrons. The device was characterized by a broadband photoresponse from 300 to 1500 nm and a photoresponse time of less than 3 ms.

Colloidal PbSe QDs can also act as efficient photocatalysts.[127, 128] For instance, Er-doped colloidal PbSe QDs were successfully used as catalysts of the photocatalytic decomposition of malachite green dye in water.[128] This dye has various applications in fish farming, exhibits teratogenic activity and should be removed from wastewater.

7. Conclusion

Recent progress in application of CQDs began with the discovery of efficient method of high-temperature colloidal synthesis. Colloidal PbSe QDs thus prepared have the first exciton absorption peak and photoluminescence in the range from 0.75 to 3.5 μm owing to the large exciton Bohr radius and narrow band gap of PbSe. This makes colloidal PbSe QDs and other lead chalcogenide QDs candidates for application in lasers, telecommunication devices, solar cells, photodetectors and electroluminescent devices. For instance, a PCE has increased from 1% for the QD first-generation solar cells to 16.6% in very recent reports.[129]

The material presented in this review gives a comprehensive overview of modern methods for the synthesis of colloidal PbSe QDs irrespective of the final field of application. Currently the most important application of PbSe is a material for photoelectric devices. Nevertheless it should be noted that nanoparticles synthesized for a certain application field can be in demand in other fields.

The state of the art in surface chemistry of colloidal PbSe QDs and related problems of the oxidative stability and conductivity of films fabricated from this type of nanoparticles are also discussed in sufficient detail. Deep insight into the mechanisms of different synthetic methods and into chemical properties of the surface of colloidal PbSe QDs should underlie the synthesis of nanoparticles with specified properties.

Figures 5 – 8 are courtesy of the American Chemical Society. Figure 3 is courtesy of Wiley-VCH Verlag. Figure 2 is courtesy of The Royal Society of Chemistry.

This review has been written within the framework of the State Assignment No. AAAA-A19-119070790003-7 and financially supported by the Russian Foundation for Basic Research (Project No. 18-29-20062) and by the Government of the Russian Federation (under Contract No. 074-02-2018-286).

References

1. M.A.Reed, J.N.Randall, R.J.Aggarwal, R.J.Matyi, T.M.Moore, A.E.Wetsel. *Phys. Rev. Lett.*, **60**, 535 (1988)
2. C.B.Murray, D.J.Norris, M.G.Bawendi. *J. Am. Chem. Soc.*, **115**, 8706 (1993)
3. P.Martyniuk, A.Rogalski. *Prog. Quantum Electron.*, **32**, 89 (2008)
4. J.S.Steckel, S.Coe-Sullivan, V.Bulović, M.G.Bawendi. *Adv. Mater.*, **15**, 1862 (2003)
5. J.M.Pietryga, J.A.Hollingsworth, F.Wang, W.E.Buhro. In *Inorganic Synthesis*. Vol. 36. (Eds G.S.Girolami, A.P.Sattelberger). (Hoboken: Wiley, 2014). P. 198
6. J.N.Zemel, J.D.Jensen, R.B.Schoolar. *Phys. Rev., A*, **140**, 330 (1965)
7. H.Zogg, A.Ishida. In *Infrared Detectors and Emitters: Materials and Devices. Electronic Materials Series*. Vol. 8. (Eds P.Capper, C.T.Elliott). (Boston, MA: Springer Science, 2001). P. 43
8. A.Rogalski. *Prog. Quantum Electron.*, **27** (2 – 3), 59 (2003)
9. G.Vergara, M.T.Montojo, M.C.Torquemada, M.T.Rodrigo, F.J.Sánchez, L.J.Gómez, R.M.Almazán, M.Verdú, P.Rodríguez, V.Villamayor, M.Álvarez, J.Diezhandino, J.Plaza, I.Catalán. *Opto-Electron. Rev.*, **15**, 110 (2007)
10. S.Anders, G.Strasser, E.Gornik. In *Handbook of Laser Technology and Applications*. Vol. 2. (Eds C.E.Webb, J.D.C.Jones). (Institute of Physics Publishing, 2004). P. 692
11. D.V.Talapin, C.B.Murray. *Science,* **310**, 86 (2005)
12. R.Schaller, V.Klimov. *Phys. Rev. Lett.*, **92**, 186601 (2004)
13. R.J.Ellingson, M.C.Beard, J.C.Johnson, P.Yu, O.I.Micic, A.J.Nozik, A.Shabaev, A.L.Efros. *Nano Lett.*, **5**, 865 (2005)
14. M.Kumar, S.Vezzoli, Z.Wang, V.Chaudhary, R.V.Ramanujan, G.G.Gurzadyan, A.Bruno, C.Soci. *Phys. Chem. Chem. Phys.*, **18**, 31107 (2016)
15. W.Shockley, H.J.Queisser. *J. Appl. Phys.*, **32**, 510 (1961)
16. L.M.Nikolenko, V.F.Razumov. *Russ. Chem. Rev.*, **82**, 429 (2013)
17. W.-T.Wu, H.Liu, C.Dong, W.-J.Zheng, L.-L.Han, L.Li, S.-Z.Qiao, J.Yang, X.-W.Du. *Langmuir*, **31**, 2251 (2015)
18. S.B.Brichkin, V.F.Razumov. *Russ. Chem. Rev.*, **85**, 1297 (2016)
19. I.Moreels, K.Lambert, D.De Muynck, F.Vanhaecke, D.Poelman, J.C.Martins, G.Allan, Z.Hens. *Chem. Mater.*, **19**, 6101 (2007)

20. Q.Dai, Y.Wang, X.Li, Y.Zhang, D.J.Pellegrino, M.Zhao, B.Zou, J.Seo, Y.Wang, W.W.Yu. *ACS Nano*, **3**, 1518 (2009)
21. G.Zaiats, D.Yanover, R.Vaxenburg, J.Tilchin, A.Sashchiuk, E.Lifshitz. *Materials*, **7**, 7243, (2014)
22. H.Fu, S.-W.Tsang. *Nanoscale*, **4**, 2187 (2012)
23. C.Gayner, K.K.Kar, W.Kim. *Mater. Today Energy,* **9**, 359 (2018)
24. J.Pichaandi, F.C.J.M.van Veggel. *Coord. Chem. Rev.*, **263** – **264**, 138 (2014)
25. J.W.Stouwdam, J.Shan, F.C.J.M.van Veggel, A.G.Pattantyus-Abraham, J.F.Young, M.Raudsepp. *J. Phys. Chem. C*, **111**, 1086 (2007)
26. C.B.Murray, S.Sun, W.Gaschler, H.Doyle, T.A.Betley, C.R.Kagan. *IBM J. Res. Dev.*, **45**, 47 (2001)
27. W.Lu, J.Fang, K.L.Stokes, J.Lin. *J. Am. Chem. Soc.*, **126**, 11798 (2004)
28. E.G.Mart'yanova, S.B.Brichkin, M.G.Spirin, V.F.Razumov. *High Energy Chem.*, **51**, 350 (2017)
29. M.G.Spirin, S.B.Brichkin, V.F.Razumov. *Russ. Chem. Bull., Int. Ed.,* **65**, 1902 (2016)
30. J.S.Steckel, B.K.H.Yen, D.C.Oertel, M.G.Bawendi. *J. Am. Chem. Soc.*, **128**, 13032 (2006)
31. C.M.Evans, M.E.Evans, T.D.Krauss. *J. Am. Chem. Soc.*, **132**, 10973 (2010)
32. K.Yu, X.Liu, Q.Zeng, D.M.Leek, J.Ouyang, K.M.Whitmore, J.A.Ripmeester, Y.Tao, M.Yang. *Angew. Chem., Int. Ed.*, **52**, 4823 (2013)
33. R.K.Čapek, D.Yanover, E.Lifshitz. *Nanoscale*, **7**, 5299 (2015)
34. L.M.De Leon Covian, J.A.Arizpe Zapata, M.A.Garza Navarro, D.I.Garcia Gutierrez. *Chalcogen. Lett.*, **11**, 567 (2014)
35. J.Joo, J.M.Pietryga, J.A.McGuire, S.-H.Jeon, D.J.Williams, H.-L.Wang, V.I.Klimov. *J. Am. Chem. Soc.*, **131**, 10620 (2009)
36. L.Lian, Y.Xia, C.Zhang, B.Xu, L.Yang, H.Liu, D.Zhang, K.Wang, J.Gao, J.Zhang. *Chem. Mater.*, **30**, 982 (2018)
37. J.Ouyang, C.Schuurmans, Y.Zhang, R.Nagelkerke, X.Wu, D.Kingston, Z.Y.Wang, D.Wilkinson, C.Li, M.Leek, Y.Tao, K.Yu. *ACS Appl. Mater. Interfaces*, **3**, 553 (2011)
38. C.M.Evans, L.Guo, J.J.Peterson, S.Maccagnano-Zacher, T.D.Krauss. *Nano Lett.*, **8**, 2896 (2008)
39. J.M.Pietryga, R.D.Schaller, D.Werder, M.H.Stewart, V.I.Klimov, J.A.Hollingsworth. *J. Am. Chem. Soc.*, **126**, 11752 (2004)
40. L.C.Frenette, T.D.Krauss, D.Todd. *Nat. Commun.*, **8**, Art. Í2082 (2017)
41. Y.-H.Liu, F.Wang, Y.Wang, P.C.Gibbons, W.E.Buhro. *J. Am. Chem. Soc.*, **133**, 17005, (2011)
42. J.E.Murphy, M.C.Beard, A.G.Norman, S.P.Ahrenkiel, J.C.Johnson, P.Yu, O.I.Mićić, R.J.Ellingson, A.J.Nozik. *J. Am. Chem. Soc.*, **128**, 3241 (2006)
43. K.-S.Cho, D.V.Talapin, W.Gaschler, C.B.Murray. *J. Am. Chem. Soc.*, **127**, 7140 (2005)
44. C.Li, T.Bai, F.Li, L.Wang, X.Wu, L.Yuan, Z.Shi, S.Feng. *CrystEngComm*, **15**, 597 (2013)
45. D.Baranov, M.J.Lynch, A.C.Curtis, A.R.Carollo, C.R.Douglass, A.M.Mateo-Tejada, D.M.Jonas. *Chem. Mater.*, **31**, 1223 (2019)
46. B.Hou, D.Benito-Alifonso, N.Kattan, D.Cherns, M.C.Galan, D.J.Fermin. *Chem. – Eur. J.*, **19**, 15847 (2013)
47. J.W.Thomson, K.Nagashima, P.M.Macdonald, G.A.Ozin. *J. Am. Chem. Soc.*, **133**, 5036 (2011)
48. L.Cademartiri, J.Bertolotti, R.Sapienza, D.S.Wiersma, G.von Freymann, G.A.Ozin. *J. Phys. Chem. B*, **110**, 671 (2006)
49. T.-M.Wang, B.Gao, Q.Wang, M.Zhao, K.-B.Kang. *Chem. – Asian J.*, **8**, 912 (2013)
50. Y.Pan, M.A.Sohel, L.Pan, Z.Wei, H.Bai, M.C.Tamargo, R.John. *Mater. Today: Proc.*, **2**, 281 (2015)
51. E.G.Durmusoglu, Y.Turker, H.Y.Acar. *J. Phys. Chem. C*, **121**, 12407 (2017)
52. C.Bullen, J.van Embden, J.Jasieniak, J.E.Cosgriff, R.J.Mulder, E.Rizzardo, M.Gu, C.L.Raston. *Chem. Mater.*, **22**, 4135 (2010)
53. J.Niu, H.Shena, X.Li, W.Xu, H.Wang, L.S.Li. *Colloids Surf., A*, **406**, 38 (2012)
54. H.Shen, J.Li, H.Shang, J.Niu, W.Xu, H.Wang, F.Guo, L.S.Li. *ACS Appl. Mater. Interfaces*, **5**, 10331 (2013)
55. B.J.Beberwyck, Y.Surendranath, A.P.Alivisatos. *J. Phys. Chem. C*, **117**, 19759 (2013)
56. J.M.Luther, H.Zheng, B.Sadtler, A.P.Alivisatos. *J. Am. Chem. Soc.*, **131**, 16851 (2009)
57. P.H.C.Camargo, Y.H.Lee, U.Jeong, Z.Zou, Y.Xia. *Langmuir*, **23**, 2985 (2007)
58. J.Zhang, J.Gao, C.P.Church, E.M.Miller, J.M.Luther, V.I.Klimov, M.C.Beard. *Nano Lett.*, **14**, 6010 (2014)
59. M.Li, J.Luo, C.Fu, H.Kan, Z.Huang, W.Huang, S.Yang, J.Zhang, J.Tang, Y.Fu, H.Li, H.Liu. *Sens. Actuators, B*, **256**, 1045 (2018)
60. S.Kim, A.R.Marshall, D.M.Kroupa, E.M.Miller, J.M.Luther, S.J.M.C.Beard. *ACS Nano*, **9**, 8157 (2015)
61. C.Zhang, Y.Xia, Z.Zhang, Z.Huang, L.Lian, X.Miao, D.Zhang, M.C.Beard, J.Zhang. *Chem. Mater.*, **29**, 3615 (2017)
62. M.V.Kovalenko, D.V.Talapin, M.A.Loi, F.Cordella, G.Hesser, M.I.Bodnarchuk, W.Heiss. *Angew. Chem., Int. Ed.*, **47**, 3029 (2008)
63. J.Li, J.Xu, L.Zhao, Q.Xu, G.Fan. *Mater. Res. Bull.*, **48**, 1560 (2013)
64. A.Begum, A.Hussain, A.Rahman. *Beilstein J. Nanotechnol.*, **3**, 438 (2012)
65. V.Melnig, M.-O.Apostu, N.Foca. *J. Nanopart. Res.*, **10**, 171 (2008)
66. O.M.Primera-Pedrozo, Z.Arslan, B.Rasulev, J.Leszczynski. *Nanoscale*, **4**, 1312 (2012)
67. M.Je, H.J.Jung, R.Koutavarapu, S.J.Lee, S.H.Lee, S.K.Kim, H.C.Choi, M.Y.Choi. *Mater. Chem. Phys.*, **217**, 427 (2018)
68. M.A.Hines, G.D.Scholes. *Adv. Mater.*, **15**, 1844 (2003)
69. J.Zhang, J.Gao, E.M.Miller, J.M.Luther, M.C.Beard. *ACS Nano*, **8** (1), 614 (2014)
70. J.Akhtar, M.Akhtar, M.A.Malik, P.O'Brien, J.Raftery. *J. Am. Chem. Soc.*, **134**, 2485 (2012)
71. M.P.Campos, M.P.Hendricks, A.N.Beecher, W.Walravens, R.A.Swain, G.T.Cleveland, Z.Hens, M.Y.Sfeir, J.S.Owen. *J. Am. Chem. Soc.*, **139**, 2296 (2017)
72. O.Chen, X.Chen, Y.Yang, J.Lynch, H.Wu, J.Zhuang, Y.C.Cao. *Angew. Chem., Int. Ed.*, **47**, 8638 (2008)
73. G.Shao, G.Chen, W.Yang, T.Ding, J.Zuo, Q.Yang. *Langmuir*, **30**, 2863 (2014)
74. P.K.Khanna, N.Singh, S.Charan, A.K.Viswanath, K.R.Patil. *Mater. Res. Bull.*, **42** 1414 (2007)
75. M.A.Boles, D.Ling, T.Hyeon, D.V.Talapin. *Nat. Mater.*, **15**, 141 (2016)
76. J.Owen. *Science*, **347**, 615, (2015)
77. J.L.Peters, K.H.W.van den Bos, S.van Aert, B.Goris, S.Bals. *Chem. Mater.*, **29**, 4122 (2017)
78. N.C.Anderson, M.P.Hendricks, J.J.Choi, J.S.Owen. *J. Am. Chem. Soc.*, **135**, 18536 (2013)
79. I.Moreels, B.Fritzinger, J.C.Martins, Z.Hens. *J. Am. Chem. Soc.*, **130**, 15081 (2008)
80. Y.Gao, M.Aerts, C.S.Suchand Sandeep, E.Talgorn, T.J.Savenije, S.Kinge, L.D.A.Siebbeles, A.J.Houtepen. *ACS Nano*, **6**, 11, 9606 (2012)
81. M.Law, J.M.Luther, Q.Song, B.K.Hughes, C.L.Perkins, A.J.Nozik. *J. Am. Chem. Soc.*, **130**, 5974 (2008)
82. C.-Y.Kuo, M.-S.Su, C.-S.Ku, S.-M.Wang, H.-Y.Lee, K.-H.Wei. *J. Mater. Chem.*, **21**, 11605 (2011)
83. G.I.Koleilat, L.Levina, H.Shukla, S.H.Myrskog, S.Hinds, A.G.Pattantyus-Abraham, E.H.Sargent. *ACS Nano*, **2**, 833 (2008)
84. M.H.Zarghami, Y.Liu, M.Gibbs, E.Gebremichael, C.Webster, M.Law. *ACS Nano*, **4**, 2475 (2010)

85. A.R.Smith, W.Yoon, W.B.Heuer, S.I.M.Baril, J.E.Boercker. *J. Phys. Chem. C*, **116**, 6031 (2012)
86. I.C.Baek, S.I.Seok, N.C.Pramanik, S.Jana, M.A.Lim, B.Y.Ahn, C.J.Lee, Y.J.Jeong. *J. Colloid Interface Sci.*, **310**, 163 (2007)
87. Y.Liu, M.Gibbs, J.Puthussery, S.Gaik, R.Ihly, H.W.Hillhouse, M.Law. *Nano Lett.*, **10**, 1960 (2010)
88. J.M.Luther, M.Law, Q.Song, C.L.Perkins, M.C.Beard, A.J.Nozik. *ACS Nano*, **2**, 271 (2008)
89. G.Sarasqueta, K.R.Choudhury, F.So. *Chem. Mater.*, **22**, 3496 (2010)
90. B.K.Hughes, D.A.Ruddy, J.L.Blackburn, D.K.Smith, M.R.Bergren, A.J.Nozik, J.C.Johnson, M.C.Beard. *ACS Nano*, **6**, 5498 (2012)
91. A.Nag, M.V.Kovalenko, J.-S.Lee, W.Liu, B.Spokoyny, D.V.Talapin. *J. Am. Chem. Soc.*, **133**, 10612 (2011)
92. D.Yang, C.Lu, H.Yin, I.P.Herman. *Nanoscale*, **5**, 7290 (2013)
93. Y.Liu, J.Tolentino, M.Gibbs, R.Ihly, C.L.Perkins, Y.Liu, N.Crawford, J.C.Hemminger, M. Law. *Nano Lett.*, **13**, 1578 (2013)
94. H.Zhang, B.Hu, L.Sun, R.Hovden, F.W.Wise, D.A.Muller, R.D.Robinson. *Nano Lett.*, **11**, 5356 (2011)
95. J.Y.Woo, J.-H.Ko, J.H.Song, K.Kim, H.Choi, Y.-H.Kim, D.C.Lee, S.Jeong. *J. Am. Chem. Soc.*, **136**, 8883 (2014)
96. C.Fu, H.Wang, T.Song, L.Zhang, W.Li, B.He, M.Sulaman, S.Yang, B.Zou. *Nanotechnology*, **27**, 065201, (2015)
97. Z.Zhang, J.Yang, X.Wen, L.Yuan, S.Shrestha, J.A.Stride, G.J.Conibeer, R.J.Patterson, S.Huang. *J. Phys. Chem. C*, **119**, 24149 (2015)
98. Q.Lin, H.J.Yun, W.Liu, H.-J.Song, N.S.Makarov, O.Isaienko, T.Nakotte, G.Chen, H.Luo, V.I.Klimov, J.M.Pietryga. *J. Am. Chem. Soc.*, **139**, 6644, (2017)
99. A.T.Fafarman, W.-K.Koh, B.T.Diroll, D.K.Kim, D.-K.Ko, S.J.Oh, X.Ye, V.Doan-Nguyen, M.R.Crump, D.C.Reifsnyder, C.B.Murray, C.R.Kagan. *J. Am. Chem. Soc.*, **133**, 15753 (2011)
100. A.G.Dong, X.C.Ye, J.Chen, Y.J.Kang, T.Gordon, J.M.Kikkawa, C.B.Murray. *J. Am. Chem. Soc.*, **133**, 998 (2011)
101. E.L.Rosen, R.Buonsanti, A.Llordes, A.M.Sawvel, D.J.Milliron, B.A.Helms. *Angew. Chem., Int. Ed.*, **51**, 684 (2012)
102. A.Hassinen, I.Moreels, K.De Nolf, P.F.Smet, J.C.Martins, Z.Hens. *J. Am. Chem. Soc.*, **134**, 20705 (2012)
103. A.W.Wills, M.Sung Kang, A.Khare, W.L.Gladfelter, D.J.Norris. *ACS Nano*, **4**, 4523 (2010)
104. E.Lifshitz, M.Brumer, A.Kigel, A.Sashchiuk, M.Bashouti, M.Sirota, E.Galun, Z.Burshtein, A.Q.Le Quang, I.Ledoux-Rak, J.Zyss. *J. Phys. Chem. B*, **110**, 25356 (2006)
105. M.Brumer, A.Kigel, L.Amirav, A.Sashchiuk, O.Solomesch, N.Tessler, E.Lifshitz. *Adv. Funct. Mater.*, **15**, 1111 (2005)
106. W.Ma, J.M.Luther, H.M.Zheng, Y.Wu, A.P.Alivisatos. *Nano Lett.*, **9**, 1699 (2009)
107. T.Song, H.Cheng, C.Fu, B.He, W.Li, J.Xu, Y.Tang, S.Yang, B.Zou. *Nanotechnology*, **27**, 165202 (2016)
108. D.K.Smith, J.M.Luther, O.E.Semonin, A.J.Nozik, M.C.Beard. *ACS Nano*, **5**, 183 (2011)
109. G.Shao, G.Chen, J.Zuo, M.Gong, Q.Yang. *Langmuir*, **30**, 7811 (2014)
110. X.Zhu, Z.Liu, G.Shi, J.Gu, W.Wang, W.Ma. *J. Mater. Sci. Technol.*, **33**, 418 (2017)
111. S.A.Saah, M.D.Khan, P.D.McNaughter, J.A.M.Awudza, N.Revaprasadu, P.O'Brien. *New J. Chem.*, **42**, 16602 (2018)
112. C.Zhang, X.Fu, Z.Peng, J.Gao, Y.Xia, J.Zhang, W.Luo, H.Li, Y.Wang, D.Zhang. *CrystEngComm*, **20**, 2519 (2018)
113. W.Shi, S.W.H.Eijt, C.S.S.Sandeep, L.D.A.Siebbeles, A.J.Houtepen, S.Kinge, E.Bruck, B.Barbiellini, A.Bansil. *Appl. Phys. Lett.*, **108**, 081602 (2016)
114. M.Sykora, A.Y.Koposov, J.A.McGuire, R.K.Schulze, O.Tretiak, J.M.Pietryga, V.I.Klimov. *ACS Nano*, **4**, 2021 (2010)
115. C.Gautier, M.Cambon-Muller, M.Averous. *Appl. Surf. Sci.*, **141**, 157 (1999)
116. H.-M.So, J.Y.Woo, S.Jeong, W.S.Chang. *Opt. Mater. Express*, **7**, 2905 (2017)
117. Y.Zhang, C.Ding, G.Wu, N.Nakazawa, J.Chang, Y.Ogomi, T.Toyoda, S.Hayase, K.Katayama, Q.Shen. *J. Phys. Chem. C*, **120**, 28509 (2016)
118. W.K.Bae, J.Joo, L.A.Padilha, J.Won, D.C.Lee, Q.Lin. *J. Am. Chem. Soc.*, **134**, 20160 (2012)
119. X.Lan, O.Voznyy, A.Kiani, F.P.G.de Arquer, A.S.Abbas, G.-H.Kim, M.Liu, Z.Yang, G.Walters, J.Xu, M.Yuan, Z.Ning, F.Fan, P.Kanjanaboos, I.Kramer, D.Zhitomirsky, P.Lee, A.Perelgut, S.Hoogland, E.H.Sargent. *Adv. Mater.*, **28**, 299 (2016)
120. A.R.Marshall, M.R.Young, A.J.Nozik, M.C.Beard, J.M.Luther. *J. Phys. Chem. Lett.*, **6**, 2892 (2015)
121. J.Y.Woo, S.Lee, S.Lee, W.D.Kim, K.Lee, K.Kim, H.J.An, D.C.Lee, S.Jeong. *J. Am. Chem. Soc.*, **138**, 876 (2016)
122. Z.Zhang, Z.Chen, L.Yuan, W.Chen, J.Yang, B.Wang, X.Wen, J.Zhang, L.Hu, J.A.Stride, G.J.Conibeer, R.J.Patterson, S.Huang. *Adv. Mater.*, **29**, 1703214 (2017)
123. H.Wang, Z.Li, C.Fu, D.Yang, L.Zhang, S.Yang, B.Zou. *IEEE Photon. Technol. Lett.*, **27**, 612 (2015)
124. Z.Jiang, W.Hu, C.Mo, Y.Liu, W.Zhang, G.You, L.Wang, M.R.M.Atalla, Y.Zhang, J.Liu, K.K.Kurhade, J.Xu. *Nanoscale*, **7**, 16195 (2015)
125. X.Xing, C.Liu, W.Shang, H.Qin, Z.Chen, F.Cao. *Infrared Phys. Technol.*, **98**, 315 (2019)
126. Y.Yu, Y.Zhang, Z.Zhang, H.Zhang, X.Song, M.Cao, Y.Che, H.Dai, J.Yang, J.Wang, H.Zhang, J.Yao. *J. Phys. Chem. Lett.*, **8**, 445 (2017)
127. Z.Györi, Z.Kónya, Á.Kukovecz. *Appl. Catal. B: Environmental.*, **179**, 583 (2015)
128. A.Khataeea, S.Arefi-Oskoui, M.Fathiniaa, A.Esmaeili. *J. Mol. Catal. A: Chem.*, **398**, 255 (2015)
129. *Best Research-Cell Eféciency Chart*. https://www.nrel.gov/pv/cell-efficiency.html (Last accessed 29.01.2020)